

TECHNICAL NOTE

D-1494

THE LOWER BOUND OF ATTAINABLE SONIC-BOOM OVERPRESSURE
AND DESIGN METHODS OF APPROACHING THIS LIMIT

By Harry W. Carlson

Langley Research Center
Langley Station, Hampton, Va.

NATIONAL AERONAUTICS AND SPACE ADMINISTRATION
WASHINGTON

October 1962

NATIONAL AERONAUTICS AND SPACE ADMINISTRATION

TECHNICAL NOTE D-1494

THE LOWER BOUND OF ATTAINABLE SONIC-BOOM OVERPRESSURE
AND DESIGN METHODS OF APPROACHING THIS LIMIT

By Harry W. Carlson

SUMMARY

From a study of existing sonic-boom theory it has been possible to establish an approximate lower bound of attainable sonic-boom overpressure, which depends only on the airplane length, weight, and volume and on the flight conditions. This lower bound may be approached over a narrow range of flight conditions through the application of appropriate design considerations. In general, for intermediate values of lift coefficient the major portion of the lift generating surfaces must be located aft of the maximum cross-sectional area, whereas for higher values of lift coefficient the maximum area must be well forward and/or the lift-producing surfaces must extend well toward the airplane nose.

INTRODUCTION

In view of the severity of the sonic-boom problem, particularly with reference to the supersonic transport, it is possible that configuration choice may depend to some degree on the sonic-boom characteristics. The available theory of references 1 and 2 provides a useful tool for a sonic-boom analysis of configurations under study. Although detailed calculations can be made for specific designs, it is of value to establish, in general, those features which exert the greatest influence and to point out design considerations which tend to minimize the problem. The purpose of this paper is to establish a lower bound of attainable sonic-boom overpressure and to discuss design requirements for approaching this limiting value.

SYMBOLS

- $A(t)$ cross-sectional area of airplane at station $x = t$
- A_b cross-sectional area at base of airplane (station $x = l$)
- $B(t)$ equivalent cross-sectional area due to lift at station $x = t$ given
by $B(t) = \frac{\beta}{2q} \int_0^t F_L' dt$

C_L	lift coefficient
D_b	equivalent diameter at base of airplane (station $x = l$), $\sqrt{\frac{l}{\pi}} A_b$
$F(\tau)$	area distribution function (see eq. (2))
F_L'	lifting force per unit length along airplane longitudinal axis
h	airplane flight altitude
K_r	reflection factor
K_s	effective-area-distribution shape factor
l	length of airplane
M	Mach number
p	reference pressure
p_a	atmospheric pressure at altitude
p_g	atmospheric pressure at ground
q	free-stream dynamic pressure
R	parameter used in describing the shape of a family of effective-area-distribution curves (see eq. (3))
S	wing planform area
T_0	root of equation $F(\tau) = 0$ that gives largest positive value for integral $\int_0^{T_0} F(\tau) d\tau$
t, τ	dummy variables of integration, measured in same direction and using same units as x
V	volume of airplane
W	weight of airplane
x	distance measured rearward along airplane longitudinal axis from nose
$\beta = \sqrt{M^2 - 1}$	
γ	ratio of specific heats, for air 1.4

A prime is used to indicate a first derivative and a double prime is used to indicate a second derivative with respect to distance.

ANALYSIS AND DISCUSSION OF RESULTS

The sonic-boom theory of references 1 and 2 has shown a reasonable agreement with the flight measurements of references 3 to 7 and the wind-tunnel measurements of references 8, 9, and 10. Equation (1) derived from reference 2 gives the pressure rise at the bow shock in a uniform atmosphere as

$$\frac{\Delta p}{p} = \frac{K_r}{h^{3/4}} \frac{\gamma(2\beta)^{1/4}}{\sqrt{\gamma+1}} \sqrt{\int_0^{T_0} F(\tau) d\tau} \quad (1)$$

The reflection factor K_r depends on the nature of the surface on which the measurements are made. A value of K_r of 2.0 corresponding to complete reflection on smooth and level ground has been assumed for all the calculations made in this report. The integration limit T_0 is that root of the equation $F(\tau) = 0$ which gives the largest positive value for the integral. The function $F(\tau)$ depends on the longitudinal distribution of the cross-sectional area and lift of the airplane and is defined as

$$F(\tau) = \frac{1}{2\pi} \int_0^\tau \frac{[A(t) + B(t)]''}{\sqrt{\tau - t}} dt \quad (2)$$

The $F(\tau)$ function as used herein differs from the original form presented in reference 2 in that the area and lift contributions are combined in a single equation rather than being treated separately. Direct addition of the area and lift functions has been made possible by expressing the lift in terms of the accumulated or integrated lift $\int F_L' dt$ rather than the loading distribution F_L' .

Sonic-boom strength thus depends on the manner in which the actual cross-sectional area combines with a fictitious or equivalent area due to lift as illustrated in figure 1. The cross-sectional area $A(t)$ reduces to zero or nearly zero at the base of the airplane, depending on the jet exit and wake conditions assumed. The equivalent area due to lift $B(t)$ however reaches a maximum at the base. This maximum value of $B(t)$ is equal to $\frac{\beta}{2} C_{LS}$ or in other terms $\frac{\beta}{2} \frac{W}{q}$ and, thus, in level flight depends only on the weight of the airplane and the flight conditions. The sonic-boom overpressure is calculated by performing the indicated operations of equations (1) and (2) on the effective area distribution obtained by a direct addition of the $A(t)$ and $B(t)$ curves.

If it is assumed that the configuration area and lift distributions are independent and can be varied at will, the possibility of the existence of an optimum $A + B$ area distribution corresponding to minimum boom strength can be explored. For purposes of illustration a family of arbitrary effective-area-distribution curves has been formed by assigning various values to the parameter R in the following equation:

$$\frac{A(t) + B(t)}{A_b + \frac{\beta}{2} C_L S} = R \left(\frac{t}{l} \right)^2 - (R - 1) \left(\frac{t}{l} \right)^3 \quad (3)$$

Three of the effective-area-distribution curves in this family are shown in figure 2. As a matter of interest, the area distribution of a minimum-drag body of given length and given base area as defined by Von Kármán in reference 11 has also been shown.

Values of sonic-boom overpressure for the family of curves can be determined by substituting equation (3) into equations (1) and (2). The resulting expression is given by

$$\frac{\Delta p}{p} = \frac{K_S K_R \beta^{1/4}}{\left(\frac{h}{l} \right)^{3/4}} \sqrt{\frac{A_b}{l^2} + \frac{\beta}{2} C_L \frac{S}{l^2}} \quad (4)$$

where K_S is an effective-area-distribution shape factor which depends upon the value of R according to the following relations:

$$K_S = 1.21 \sqrt{\frac{R}{3} - \frac{2(R - 1)}{5}} \quad (R < 2) \quad (5a)$$

and

$$K_S = 0.72 \sqrt{\frac{R \left(\frac{R}{R - 1} \right)^{3/2}}{3} - \frac{R - 1}{5} \left(\frac{R}{R - 1} \right)^{5/2}} \quad (R > 2) \quad (5b)$$

Sonic-boom strength represented by the factor K_S is given as a function of the parameter R in figure 3. A boom minimum ($K_S = 0.61$) occurs for a value of R between 2 and 3.

Equation (4) has general application and is not restricted to this one family of effective-area-distribution shapes. Every $A + B$ curve may be assigned a shape factor K_S evaluated in a similar manner. For example, the area of distribution of the Von Kármán minimum-drag body has a K_S value of 0.60. It is expected on the basis of investigations of various other families of curves, for which no lower values of K_S were found, that an absolute minimum value for the factor K_S would not be much less than 0.60. Even when the lift is zero, the

minimum boom strength body still has the same general characteristics as indicated herein. (See, for example, fig. 3 of ref. 12.)

By assuming a value of 0.60 for the effective-area-distribution shape factor, an approximate lower bound of sonic-boom intensity may be established. If an optimum combination of area and lift is assumed with no restrictions on the minimum volume and with $A_b = 0$, the lower bound may be expressed as

$$\frac{\Delta p}{p} = \frac{0.60 K_r \beta^{1/4}}{\left(\frac{h}{l}\right)^{3/4}} \sqrt{\frac{\beta}{2} C_L \frac{S}{l^2}} \quad (6)$$

This approximate lower bound depends only on the airplane length and weight and on the flight conditions. Attainment of this lower bound is dependent on having, for all flight conditions, an optimum $A + B$ curve similar to that for the area distribution of the Von Kármán minimum-drag body. This implies a rubberized airplane concept, that is, an airplane configuration whose geometry may be varied as needed to satisfy the requirements for achieving an optimum $A + B$ curve. Equation (6) is similar in form to the Whitham equation for bodies of revolution (ref. 1, p. 108), with the fineness-ratio term of that equation being replaced

by the term $\sqrt{\frac{\beta}{2} C_L \frac{S}{l^2}}$.

As the lift coefficient approaches zero, it is no longer possible for the optimum combination to contain the necessary airplane volume. Thus, it is necessary to introduce a volume restraint. When only the area distribution $A(t)$ is considered, the volume-restraint lower bound may be expressed as

$$\frac{\Delta p}{p} = \frac{0.60 K_r \beta^{1/4}}{\left(\frac{h}{l}\right)^{3/4}} \sqrt{\frac{A_b}{l^2}} \quad (7a)$$

or

$$\frac{\Delta p}{p} = \frac{0.53 K_r \beta^{1/4}}{\left(\frac{h}{l}\right)^{3/4}} \frac{D_b}{l} \quad (7b)$$

Except for the value of the constant and the inclusion of the reflection factor, equation (7b) is the same as the Whitham equation for bodies of revolution but is restricted to the condition where the maximum area or equivalent diameter occurs at the base. The lower-bound body shape factor of 0.53 used here compares with a value of 0.64 for a closed parabolic body. For the Von Kármán minimum-drag-body area distribution the lower bound of boom intensity may be expressed as a function of volume as follows:

$$\frac{\Delta p}{p} = \frac{0.83 K_r \beta^{1/4}}{\left(\frac{h}{l}\right)^{3/4}} \sqrt{\frac{V}{l^3}} \quad (8)$$

Equation (8) is used in establishing the volume restraint.

The approximate sonic-boom lower bound is shown in figure 4 as a function of a lift parameter. As an example, a volume restraint has been applied for a value of V/l^3 representative of that for supersonic-transport configurations. Also in this figure are sketches of A and A + B distributions that meet the fixed-volume ($V = 0.0027l^3$) and boom-minimization requirements of an optimum combination of area and lift distributions. Above these plots are representative thin-wing configurations with uniform loading which satisfy the area- and lift-distribution requirements. For intermediate values of lift coefficient the major portion of the lift generating surfaces must be located aft of the maximum cross-sectional area. This result is in general agreement with the observations made in reference 13. However, for higher values of lift coefficient the maximum area must be well forward and/or the wing must extend well toward the airplane nose in order to obtain an optimum A + B shape.

The lower bound can not be attained throughout the lift-coefficient range with a fixed design. From a practical standpoint, however, this lower bound may be approached over a limited range of lifting conditions through proper design. Figure 5 illustrates the application of boom-minimization concepts to a supersonic-transport design. Sonic-boom ground overpressures for a Mach number of 3.0 have been plotted as a function of flight altitude for two configurations representative of current supersonic-transport designs, both having a length of 190 feet, a weight of 300,000 pounds, and a volume of 18,500 cubic feet. The reference pressure p was taken to be the geometric mean of the atmospheric pressures on the ground and those at altitude $\sqrt{p_a p_g}$. Also shown in figure 5 is the approximate lower bound with and without a volume restraint. One of these configurations would have a boom level of about 1.25 pounds per square foot at a cruise altitude of 70,000 feet, a value only slightly greater than the lower bound. The other configuration, which does not meet the boom-minimization requirements, would have a boom strength some 30 percent higher at the same altitude. The A and A + B curves corresponding to level flight conditions at 70,000 feet have been shown for comparison with the corresponding calculated overpressure values.

CONCLUDING REMARKS

From a study of existing sonic-boom theory it is possible to establish an approximate lower bound of attainable sonic-boom overpressure, which depends on the airplane length, weight, and volume and on the flight conditions. This lower bound may be approached over a narrow range of flight conditions through the application of appropriate design considerations. In general, for intermediate

values of lift coefficient the major portion of the lift generating surfaces must be located aft of the maximum cross-sectional area, whereas for higher values of lift coefficient the maximum area must be well forward and/or the lift-producing surfaces must extend well toward the airplane nose.

Langley Research Center,
National Aeronautics and Space Administration,
Langley Station, Hampton, Va., July 31, 1962.

REFERENCES

1. Whitham, G. B.: The Behaviour of Supersonic Flow Past a Body of Revolution, Far From the Axis. Proc. Roy. Soc. (London), ser. A, vol. 201, no. 1064, Mar. 7, 1950, pp. 89-109.
2. Walkden, F.: The Shock Pattern of a Wing-Body Combination, Far From the Flight Path. Aero. Quarterly, vol. IX, p. 2, May 1958, pp. 164-194.
3. Mullens, Marshall E.: A Flight Test Investigation of the Sonic Boom. AFFTC-TN-56-20, Air Res. and Dev. Command, U.S. Air Force, May 1956.
4. Maglieri, Domenic J., Hubbard, Harvey H., and Lansing, Donald L.: Ground Measurements of the Shock-Wave Noise From Airplanes in Level Flight at Mach Numbers to 1.4 and at Altitudes to 45,000 Feet. NASA TN D-48, 1959.
5. Lina, Lindsay J., and Maglieri, Domenic J.: Ground Measurements of Airplane Shock-Wave Noise at Mach Numbers to 2.0 and at Altitudes to 60,000 Feet. NASA TN D-235, 1960.
6. Maglieri, Domenic J., and Hubbard, Harvey H.: Ground Measurements of the Shock-Wave Noise From Supersonic Bomber Airplanes in the Altitude Range From 30,000 to 50,000 Feet. NASA TN D-880, 1961.
7. Hubbard, Harvey H., Maglieri, Domenic J., Huckel, Vera, and Hilton, David A.: Ground Measurements of Sonic-Boom Pressures for the Altitude Range of 10,000 to 75,000 Feet. NASA TM X-633, 1962.
8. Carlson, Harry W.: An Investigation of Some Aspects of the Sonic Boom by Means of Wind-Tunnel Measurements of Pressures About Several Bodies at a Mach Number of 2.01. NASA TN D-161, 1959.
9. Carlson, Harry W.: An Investigation of the Influence of Lift on Sonic-Boom Intensity by Means of Wind-Tunnel Measurements of the Pressure Fields of Several Wing-Body Combinations at a Mach Number of 2.01. NASA TN D-881, 1961.
10. Carlson, Harry W.: Wind-Tunnel Measurements of the Sonic-Boom Characteristics of a Supersonic Bomber Model and a Correlation With Flight-Test Ground Measurements. NASA TM X-700, 1962.
11. Von Kármán, Th.: The Problem of Resistance in Compressible Fluids. R. Accad. d'Italia, Cl. Sci. Fis., Mat. e Nat., vol. XIV, 1936. (Fifth Volta Congress held in Rome, Sept. 30 - Oct. 6, 1935.)
12. Maglieri, Domenic J., and Carlson, Harry W.: The Shock-Wave Noise Problem of Supersonic Aircraft in Steady Flight. NASA MEMO 3-4-59L, 1959.
13. Morris, John: An Investigation of Lifting Effects on the Intensity of Sonic Booms. Jour. R.A.S., vol. 64, no. 598, Oct. 1960, pp. 610-616.

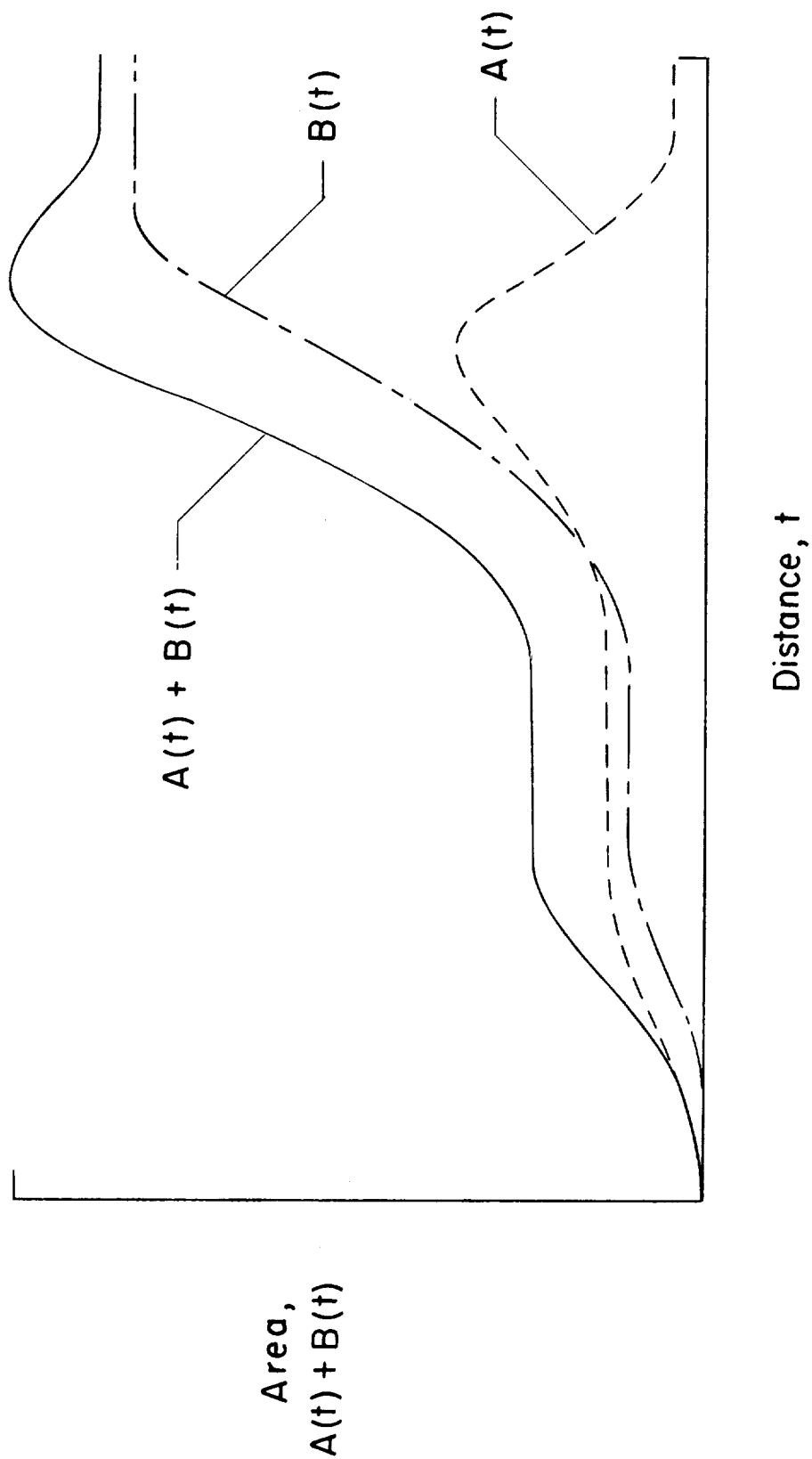
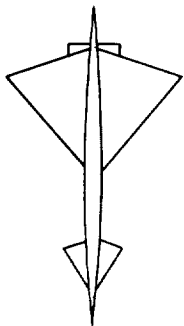


Figure 1.- An example of the contribution of area $A(t)$ and equivalent area due to lift $B(t)$ to the total effective area.

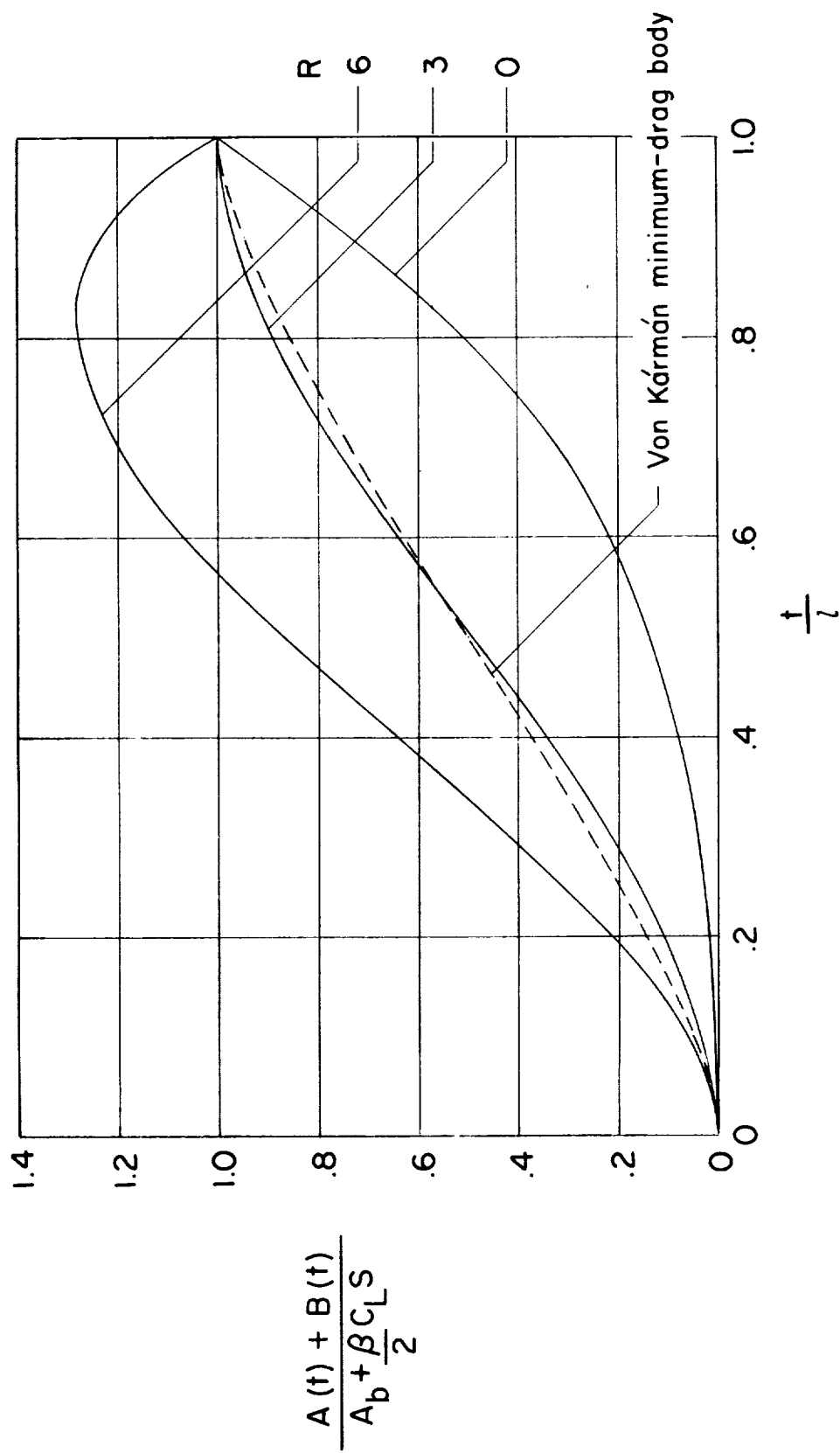


Figure 2.- Family of effective-area-distribution shapes.

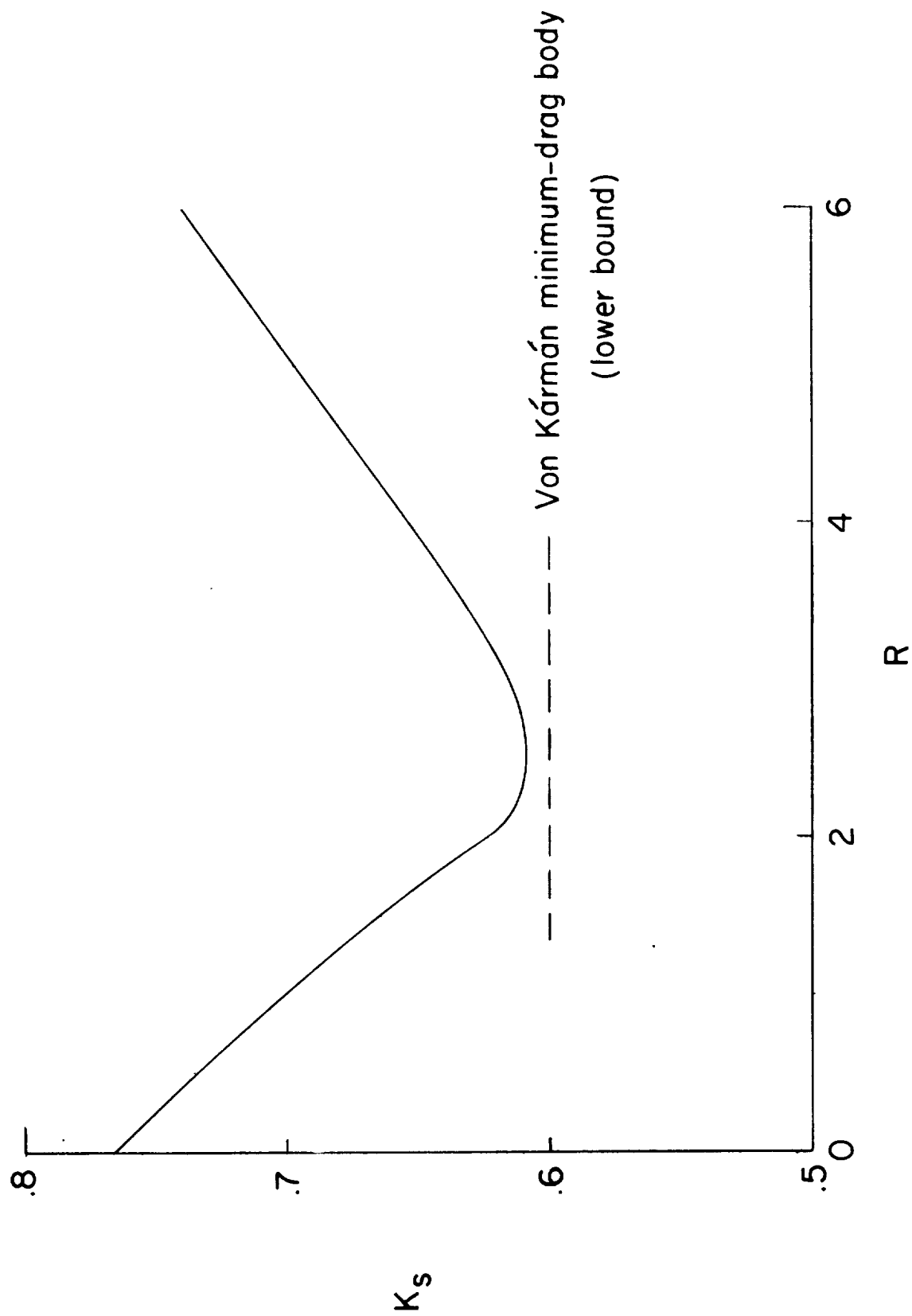


Figure 3.- Variation of sonic-boom strength parameter with effective-area-distribution shape.

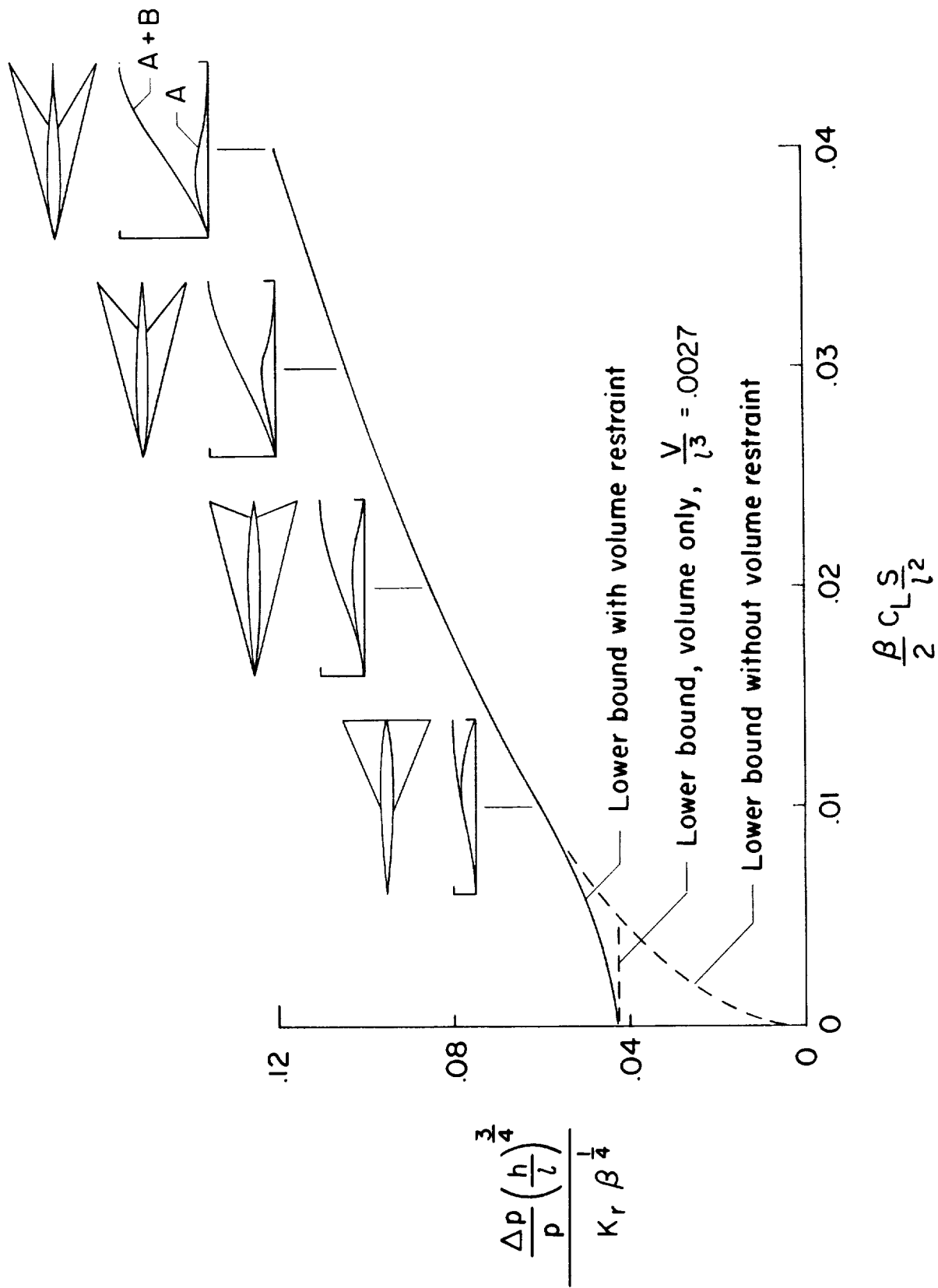


Figure 4.- Approximate sonic-boom lower bound for an optimum combination of lift and volume.

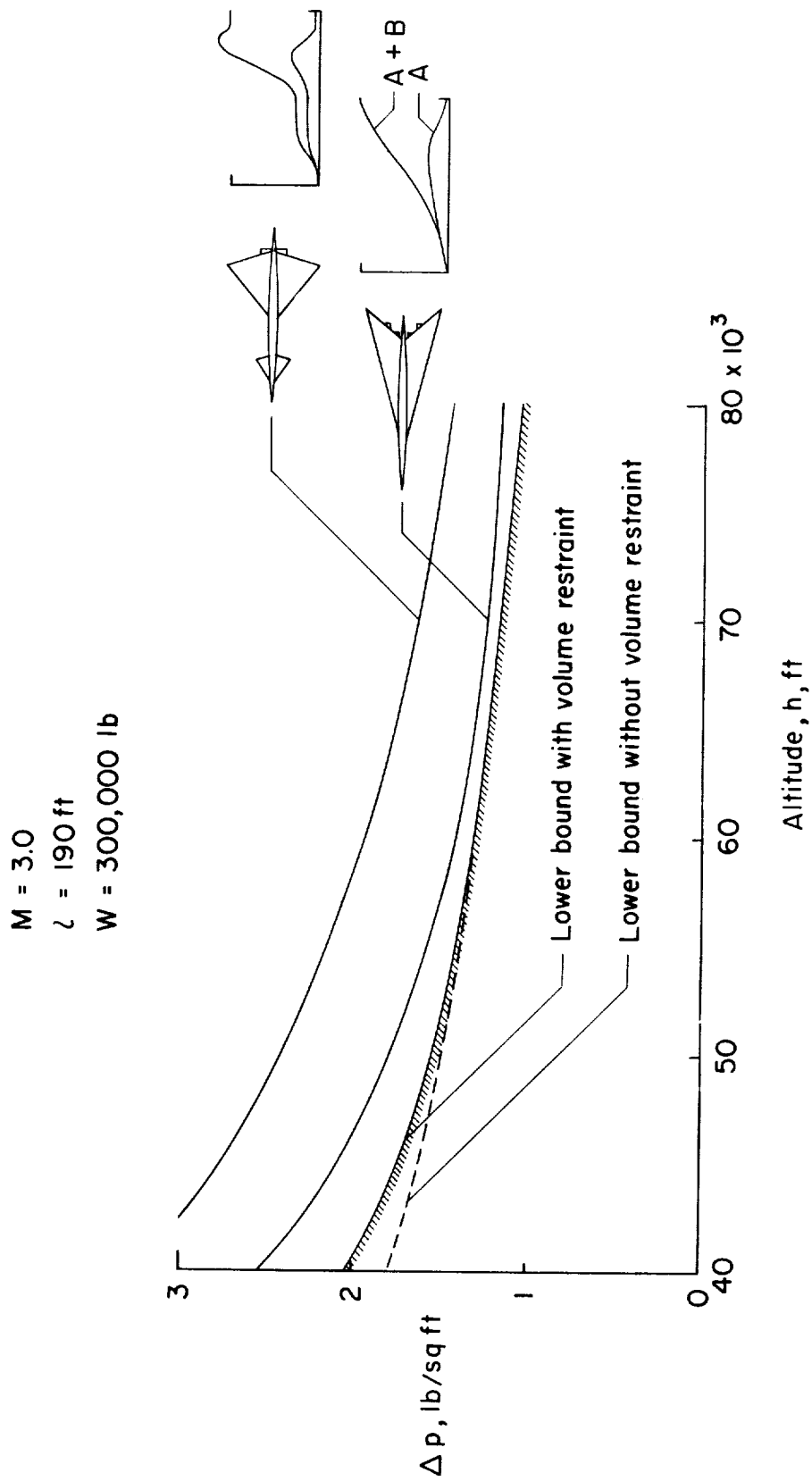


Figure 5.- Calculated sonic-boom characteristics for two supersonic-transport configurations compared with the approximate lower bound for that size and weight.

